A New Scaling for Tornado-Like Vortices

DAVID S. NOLAN

Rosenstiel School of Marine and Atmospheric Science, University of Miami, Miami, Florida

(Manuscript received 1 April 2004, in final form 19 November 2004)

ABSTRACT

A new approach is presented for the nondimensionalization of the Navier–Stokes equations for tornado-like vortices. This scaling is based on the results of recent numerical simulations and physical reasoning. The method clarifies and unifies the results of numerous earlier studies that used numerical simulations of axisymmetric incompressible flow to study tornadoes. Some examples are presented.

1. Introduction

Scaling and dimensional analysis are powerful mathematical tools for the study of physical phenomena (Barenblatt 1998). They offer two important advantages: 1) the number of parameters describing the physical problem can be reduced and 2) similar physical phenomena of different length and time scales can be directly compared.

Dimensional analysis has been used to simplify and understand the results of numerous studies of tornado-like vortices using laboratory models (Ward 1972; Wan and Chang 1972; Church et al. 1979; see the review by Church and Snow 1993) and numerical simulations (Bode et al. 1975; Rotunno 1979; Walko and Gall 1986; Howells et al. 1988; Fiedler 1993, 1994, 1998; Nolan and Farrell 1999). The most widely known result from the earlier studies, both physical and numerical, is that the structure of the low-level vortex is controlled to some extent by a dimensionless parameter known as the swirl ratio, which is the ratio of the circulation of the fluid that feeds into the vortex to the rate at which fluid flows through the vortex. However, both laboratory results (Dessens 1972; Church et al. 1979, see their Fig. 8) and numerical simulations (Walko and Gall 1986; Howells et al. 1988) demonstrated that the Reynolds number Re, which is the ratio of the flow rate to the effective viscosity (molecular or turbulent), also has an important influence on the flow structure.

A complicating factor in the earlier studies was that both the laboratory and numerical models were designed with specified inflow and outflow regions in close proximity to the vortex core. The scales of these inflow and outflow regions introduced additional dimensionless parameters into the analysis (Davies-Jones 1973; Church et al. 1979). The problem was greatly simplified by the modeling approach of Fiedler (1993), which used a much larger domain and created a tornado-like vortex by using a fixed buoyancy field to force low-level convergence of an incompressible fluid in solid-body rotation. Thus, the structure of the flow in and out of the tornado-like vortex was determined by the larger circulation, not by the arbitrarily defined boundary conditions at inflow and outflow regions. Furthermore, this advance provided a clear connection between the strength of the buoyancy field and the simulated maximum wind speeds, which allowed for a direct prediction of the expected maximum wind speeds in tornadoes, given a particular convective environment (Fiedler 1994, 1998).

Using Fiedler's approach, Nolan and Farrell (1999) explored how the intensity, structure, and behavior of tornado-like vortices depend on the model parameters: the strength of the convective forcing, the environmental rotation rate Ω, and the kinematic viscosity ν. They found that the *vortex Reynolds number*, Re_V, which is the ratio of the circulation of the fluid feeding into the low-level vortex to the viscosity, seemed to control the low-level vortex structure rather than the swirl ratio. Indeed, dimensional analysis of the simplified modeling environment suggests that Re_V is a potentially important parameter. However, its significance could only be established by examining the results of numerous (in fact, several hundred) numerical simulations with varying values of Ω and ν (see Nolan and Farrell 1999, their section 6c and Figs. 23, 24, and 25). Additional high-resolution

Corresponding author address: Prof. David S. Nolan, RSMAS/MPO, 4600 Rickenbacker Causeway, Miami, FL 33149.
E-mail: dnolan@rsmas.miami.edu

simulations by Nolan et al. (2000), using an adaptive-mesh-refinement technique, confirmed these results.

In this note we will show how the controlling influence of Re_V can indeed be determined from scaling and dimensional analysis. Furthermore, this scaling is useful because both the maximum wind speed and the radius of maximum winds will be $O(1)$ quantities. Considering the overall results of previous numerical simulations, we proceed from the following assumptions about convectively driven vortices:

1) The mean maximum azimuthal wind speed scales with, and in fact is nearly equal to, the "thermodynamic speed limit," which is the wind speed associated with the convective available potential energy (CAPE).
2) While the vertically integrated convective forcing determines the wind speed, the altitude and vertical distribution of the convective forcing do not influence the low-level flow structure.[1]
3) The *horizontal* scale of the convective forcing region does influence the low-level flow structure. This is because fluid of circulation $\Gamma \sim \Omega L^2$ is drawn into the vortex core.

2. Equations and nondimensionalization

Our starting point is the axisymmetric, incompressible Navier–Stokes equations in cylindrical coordinates, set in a reference frame that rotates at angular velocity Ω:

$$\frac{\partial u}{\partial t} + u\frac{\partial u}{\partial r} + w\frac{\partial u}{\partial z} - \frac{v^2}{r} - 2\Omega v = -\frac{1}{\rho}\frac{\partial p}{\partial r} + \frac{\mu}{\rho}\left[\frac{\partial}{\partial r}\left(\frac{1}{r}\frac{\partial}{\partial r}(ru)\right) + \frac{\partial^2 u}{\partial z^2}\right] \tag{2.1}$$

$$\frac{\partial v}{\partial t} + u\frac{\partial v}{\partial r} + w\frac{\partial v}{\partial z} + \frac{uv}{r} + 2\Omega u = \frac{\mu}{\rho}\left[\frac{\partial}{\partial r}\left(\frac{1}{r}\frac{\partial}{\partial r}(rv)\right) + \frac{\partial^2 v}{\partial z^2}\right] \tag{2.2}$$

$$\frac{\partial w}{\partial t} + u\frac{\partial w}{\partial r} + w\frac{\partial w}{\partial z} = -\frac{1}{\rho}\frac{\partial p}{\partial z} + \frac{\mu}{\rho}\left[\frac{1}{r}\frac{\partial}{\partial r}\left(r\frac{\partial w}{\partial r}\right) + \frac{\partial^2 w}{\partial z^2}\right] + F_z \tag{2.3}$$

$$\frac{1}{r}\frac{\partial}{\partial r}(ru) + \frac{\partial w}{\partial z} = 0, \tag{2.4}$$

where u is the radial velocity, v is the azimuthal velocity, w is the vertical velocity, p is the pressure, F_z is a vertical forcing term (the buoyant acceleration), ρ is the constant density, and μ is the viscosity. These equations can be nondimensionalized by

$$(u^*, v^*, w^*) = U \times (u, v, w) \tag{2.5}$$

$$(r^*, z^*) = L \times (r, z) \tag{2.6}$$

$$p^* = Pp \tag{2.7}$$

$$F_z^* = FF_z \tag{2.8}$$

$$t^* = Tt, \tag{2.9}$$

where from (2.5) and on, all dimensional variables are superscripted with an asterisk and nondimensional variables are left plain. Also from (2.5) on, nonasterisk capital letters are physical scales. One must make appropriate choices for U, L, P, F, and T. An obvious set of such choices is to set

$$L = Z^*, \tag{2.10}$$

where Z^* is the vertical extent of the domain, and

$$F = \frac{1}{L}\int_0^L F_z^*(0, z)\, dz \quad \text{(the mean vertical forcing at the axis)}, \tag{2.11}$$

$$U^2 = 2FL \text{ (the thermodynamic speed limit)} \tag{2.12}$$

$$P = \rho^* U^2, \tag{2.13}$$

$$T = \frac{L}{U} \text{(the advective time scale)}. \tag{2.14}$$

The two parameters Ω^* and μ^* are rewritten as

$$S = \frac{\Omega^* L}{U}, \tag{2.15}$$

which Nolan and Farrell (1999) identified as a kind of swirl ratio,[2] and

$$\mathrm{Re} = \frac{\rho^* UL}{\mu^*} = \frac{UL}{\nu^*}, \tag{2.16}$$

where ν^* is the dimensional kinematic viscosity, and Re is a "convective" Reynolds number (as it is based on

[1] Trapp and Davies-Jones (1997) found that the structure of the vertical forcing does control the way in which the low-level vortex forms, that is, whether it forms at the surface itself, or forms aloft and then descends to the surface (the dynamic pipe effect). They did not address the quasi-steady vortex which develops after long times.

[2] This swirl ratio is the ratio of the far-field azimuthal velocity to the maximum possible updraft speed. The definitions of swirl ratio used in earlier papers are typically the ratio of the far-field circulation to the flow rate through the vortex region, which can be related to the ratio of the azimuthal and vertical velocities, given assumptions about the size of the updraft radius and the inflow layer. These sizes are not predetermined in these large-domain simulations, so the swirl ratio given here is all that can be known from the environmental parameters alone.

the convective wind speed). Using these scalings, we obtain the nondimensional equations of motion:

$$\frac{\partial u}{\partial t} + u\frac{\partial u}{\partial r} + w\frac{\partial u}{\partial z} - \frac{v^2}{r} - 2Sv = -\frac{\partial p}{\partial r} + \frac{1}{\mathrm{Re}}\left[\frac{\partial}{\partial r}\left(\frac{1}{r}\frac{\partial}{\partial r}(ru)\right) + \frac{\partial^2 u}{\partial z^2}\right] \quad (2.17)$$

$$\frac{\partial v}{\partial t} + u\frac{\partial v}{\partial r} + w\frac{\partial v}{\partial z} + \frac{uv}{r} + 2Su = \frac{1}{\mathrm{Re}}\left[\frac{\partial}{\partial r}\left(\frac{1}{r}\frac{\partial}{\partial r}(rv)\right) + \frac{\partial^2 v}{\partial z^2}\right] \quad (2.18)$$

$$\frac{\partial w}{\partial t} + u\frac{\partial w}{\partial r} + w\frac{\partial w}{\partial z} = -\frac{\partial p}{\partial z} + \frac{1}{\mathrm{Re}}\left[\frac{1}{r}\frac{\partial}{\partial r}\left(r\frac{\partial w}{\partial r}\right) + \frac{\partial^2 w}{\partial z^2}\right] + \frac{1}{2}F_z, \quad (2.19)$$

which are essentially the equations used by Fiedler (1993, 1994, 1998) and Trapp and Davies-Jones (1997). Incompressibility (2.4) is unchanged. Nolan and Farrell (1999) and Nolan et al. (2000) used similar equations, but in a nonrotating reference frame, such that the environmental rotation was provided by initializing the flow in solid body rotation and keeping the boundary conditions rotating at the same angular velocity Ω^*. Using the equations with Coriolis terms is helpful to the present discussion because it brings the environmental rotation rate into the equations, where its influence is apparent.

For dimensional scales relevant to tornado-like vortices, we can expect the value of the nondimensional parameter S to range from 0.1 to 1, and for Re to range from 1000 to 10 000. Recall that this Reynolds number is associated with the turbulent eddy viscosity, not the molecular viscosity. This eddy viscosity value is not arbitrary, it is instead chosen so that the depth of the boundary layer and the altitude of the maximum winds are consistent with observations [e.g., Wurman et al. (1996)]. While the large values of Re suggest that the frictional terms might be small compared to the others, this is never the case in the boundary layer where the second derivatives of the velocity fields are large, ensuring a large frictional effect. Thus, we can see from the scaling (2.10)–(2.16) and the Eqs. (2.17)–(2.19) that both S and Re have a strong influence on the flow, especially in the boundary layer.

Admittedly, the interpretation of S as a swirl ratio is problematic, as there is no guarantee that $\Omega^* L$ is indicative of the azimuthal velocity in the far field, because by (2.10) L is the height of the domain. It does not necessarily indicate the distance from which fluid travels to arrive in the core of the vortex [although this was indeed the case for Fiedler (1993) and Nolan and Farrell (1999), as the height and width of the convective forcing was matched to the size of the domain in those studies].

Our new approach begins by scaling the vortex by the *expected* radius of maximum winds. We assume that parcels arriving at the location of the maximum winds have nearly conserved their circulation. This expected radius occurs where the circulation of the fluid drawn in from the far field is equal to the theoretical maximum wind speed (the thermodynamic speed limit) times its radius, therefore

$$L = \frac{\Omega^* L_r^{*2}}{U}, \quad (2.20)$$

where L_r^* is the radius of the convecting region or updraft. As before, U is scaled by the convective forcing,

$$U^2 = 2\int_0^{Z^*} F^*(0, z^*)\, dz^*. \quad (2.21)$$

The natural time scale is the vortex core circulation time

$$T = \frac{L}{U}, \quad (2.22)$$

that is, T scales with the time for a parcel to travel once around the vortex at the radius of maximum winds. The forcing is simply scaled by its maximum value, $F_{\max}$, and P is again scaled by $\rho^* U^2$. Based on the new length scale, the nondimensional rotation rate becomes

$$S = \frac{\Omega^* L}{U} = \frac{\Omega^*}{U} \times \frac{\Omega^* L_r^{*2}}{U} = \left(\frac{\Omega^* L_r^*}{U}\right)^2 \equiv S_r^2, \quad (2.23)$$

where S_r is a swirl ratio based on the horizontal scale of the convective forcing. The equations become:

$$\frac{\partial u}{\partial t} + u\frac{\partial u}{\partial r} + w\frac{\partial u}{\partial z} - \frac{v^2}{r} - 2S_r^2 v = -\frac{\partial p}{\partial r} + \frac{1}{Re_v}\left[\frac{\partial}{\partial r}\left(\frac{1}{r}\frac{\partial}{\partial r}(ru)\right) + \frac{\partial^2 u}{\partial z^2}\right] \quad (2.24)$$

$$\frac{\partial v}{\partial t} + u\frac{\partial v}{\partial r} + w\frac{\partial v}{\partial z} + \frac{uv}{r} + 2S_r^2 u = \frac{1}{Re_V}\left[\frac{\partial}{\partial r}\left(\frac{1}{r}\frac{\partial}{\partial r}(rv)\right) + \frac{\partial^2 v}{\partial z^2}\right] \quad (2.25)$$

$$\frac{\partial w}{\partial t} + u\frac{\partial w}{\partial r} + w\frac{\partial w}{\partial z} = -\frac{\partial p}{\partial z} + \frac{1}{\mathrm{Re}_V}\left[\frac{1}{r}\frac{\partial}{\partial r}\left(r\frac{\partial w}{\partial r}\right) + \frac{\partial^2 w}{\partial z^2}\right] + \gamma F_z, \quad (2.26)$$

where

$$\mathrm{Re}_V = \frac{\Omega^* L_r^{*2}}{\nu^*} \tag{2.27}$$

is the vortex Reynolds number, and the convective forcing is multiplied by the parameter

$$\gamma = \frac{LF_{\max}}{U^2}. \tag{2.28}$$

The parameter γ depends on the vertical distribution of F_z, and increases in value as the distribution becomes more localized. In much of the domain F_z is equal to zero, particularly in the boundary layer, so we would not expect the influence of γ to be significant in determining the structure of the low-level flow.

Here S_r is the ratio of the azimuthal velocity of the fluid that is brought into the vortex core $V^* \sim \Omega^* L_r^*$ to the maximum wind speed U. For scales relevant to tornado-like vortices, we can expect S_r to range in value from less than 0.1 to perhaps as much as 0.25. Since it appears squared in the equations and it is multiplied by $O(1)$ variables, the Coriolis term will usually be much smaller than the others. In this scaling, the balance between frictional and advective terms in the boundary layer is clearly controlled by Re_V.

3. Demonstration

Consider the following axisymmetric simulation with dimensional scales. The fluid is incompressible with $\rho = 1\ \mathrm{kg\ m^{-3}}$, the height of the domain is $Z^* = 6000$ m, and its maximum radius is $R^* = 6000$ m. The domain rotates at $\Omega^* = 0.005\ \mathrm{s^{-1}}$. There is a vertical forcing field at the center axis with distribution

$$F_z^*(r^*, z^*) = \begin{cases} F_{\max} \cos\left(\dfrac{\pi}{2} x^*\right), & x^* < 1 \\ 0, & x^* \geq 1, \end{cases} \tag{3.1}$$

where x^* is a modified distance from the center of the bubble,

$$x^* = \left\{ \frac{(z^* - z_b^*)^2}{L_z^{*2}} + \frac{r^{*2}}{L_r^{*2}} \right\}^{1/2}. \tag{3.2}$$

Thus, the vertical forcing field is a cosine-shaped bubble of altitude z_b^*, radius L_r^*, and depth $2L_z^*$. From (2.21), we have $U^2 = 8F_{\max} L_z^*/\pi$. We let $z_b = 3000$ m, $L_r = 1000$ m, $L_z = 2000$ m, and $F_{\max} = 1.26\ \mathrm{m\ s^{-2}}$, such that $U = 80\ \mathrm{m\ s^{-1}}$. The eddy viscosity has a constant value $\nu^* = 50\ \mathrm{m^2\ s^{-1}}$.

The axisymmetric incompressible flow model of Nolan and Farrell (1999) is used for the simulations, with 128 equally spaced grid points in the radial direction and 256 in the vertical direction; in a few cases, 512

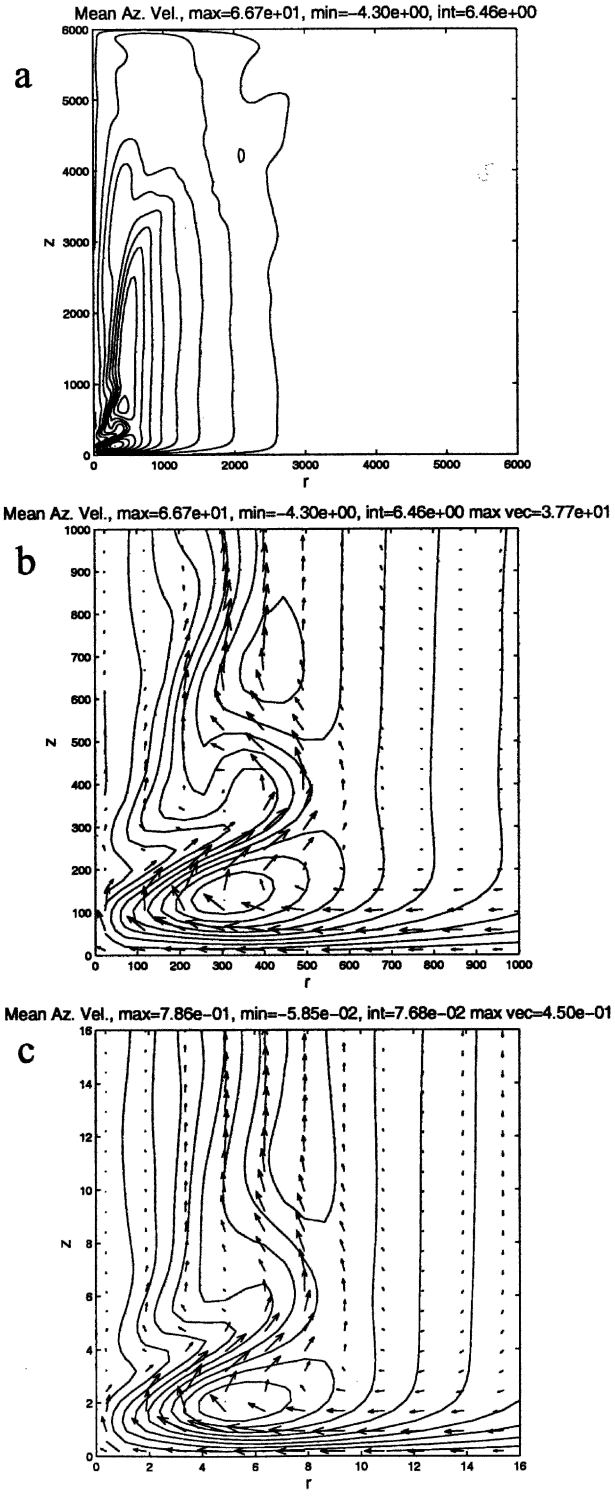

FIG. 1. Mean flow fields for a tornado-like vortex: (a) domain-scale azimuthal velocities; (b) close up of corner flow, with meridional flow vectors; and (c) a nondimensional simulation based on the same parameters. Wind speeds, contour intervals, and vector amplitudes are indicated. Units for the dimensional simulation are m and $\mathrm{m\ s^{-1}}$.

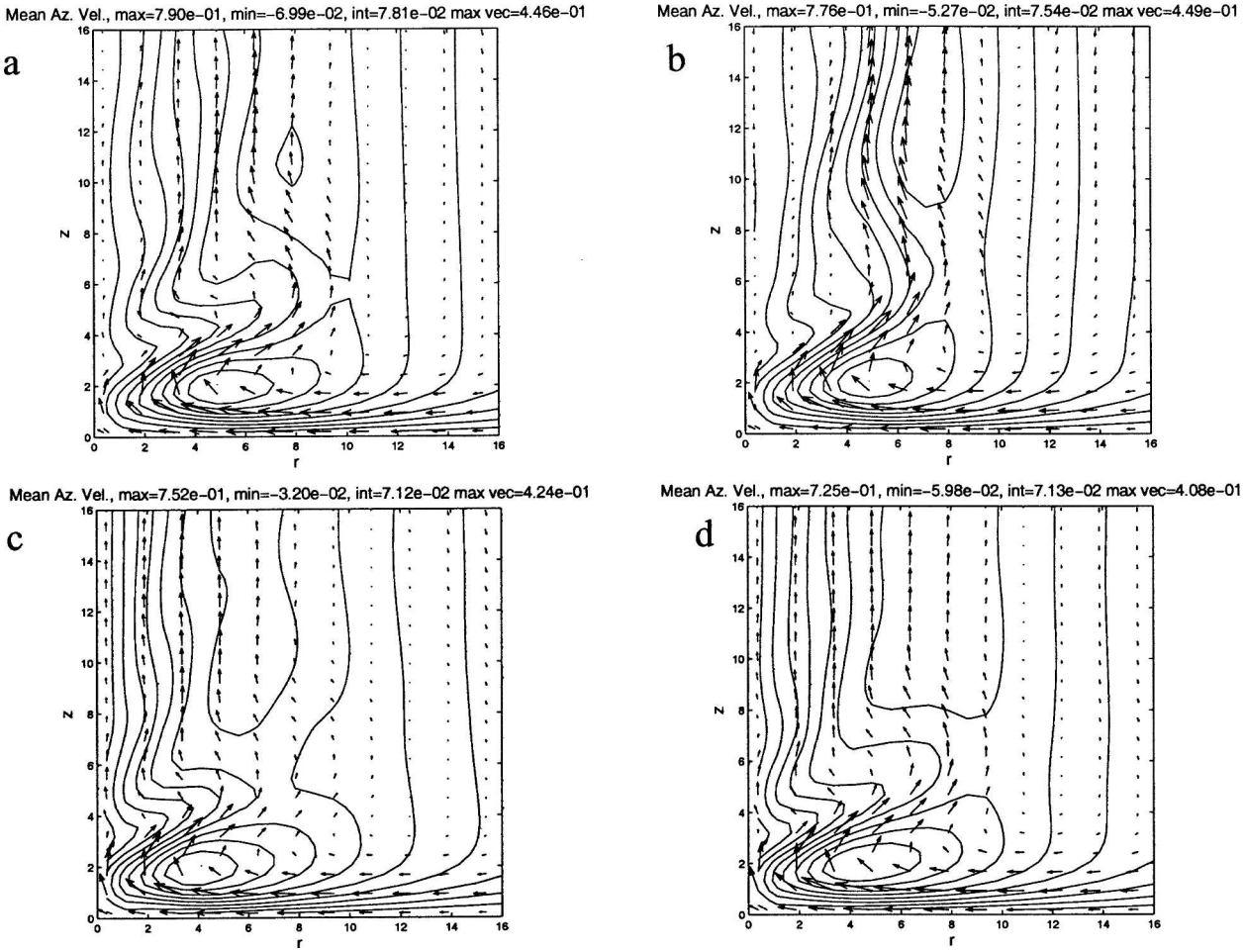

FIG. 2. Close ups of the mean corner flow for simulations using the new scaling, for different convective forcing fields: (a) for a nondimensional simulation equivalent to one with $L_z^* = 1000$ m; (b) for $L_z^* = 3000$ m; (c) for $z_c^* = 4000$ m; and (d) for three overlapping forcings as described in the text.

points were used in the vertical direction. The velocity fields every 20 seconds of the last 10 minutes from a 60-min simulation are averaged, and the result is shown in Fig. 1. The typical "drowned vortex jump" structure (Maxworthy 1972) is recovered. To be consistent with Fiedler (1993, 1994, 1998), Trapp and Davies-Jones (1997), and Eqs. (2.24)–(2.26), the velocity fields are presented in the rotating reference frame.

Using the new scaling, we have $L = 62.5$ m, $T = 0.781$ s, $\mathrm{Re}_V = 50$, and $\gamma = 0.0123$. The dimensionless distances are $Z = 96$, $R = 96$, $z_b = 48$, $L_r = 16$, $L_z = 32$. The result of an equivalent simulation, averaged as above, is shown in Fig. 1c. Unsurprisingly, the structure of the vortex is nearly identical, but we are now in a framework where the maximum azimuthal wind speed and the radius of maximum winds are $O(1)$. In fact, the radius of maximum winds are near $r = 4$, indicating that the circulation which flows into the vortex core has about four times that anticipated by (2.20). (Choosing L_r to be *twice* the horizontal scale of the convective forcing, which quadruples the value of L, results in a scaling with the radius of maximum winds at almost exactly $r = 1$.)

In section 1, it was claimed that the vertical distribution of the convective forcing function did not have a significant effect on the low-level flow structure. Figure 2 shows the results of nondimensional simulations based on dimensional parameters that have been modified to test this assertion: a) $L_z^* = 1000$ m; b) $L_z^* = 3000$ m; and c) $z_c^* = 4000$ m. In each case $F_{\max}$ (and equivalently, γ) is adjusted to keep $U = 80$ m s^{-1}. While the outflow structures are somewhat different in each case, the low-level vortex structures are nearly identical to each other and to that shown in Fig. 1. For the simulation shown in Fig. 2d, the convective forcing function was divided into three partially overlapping bubbles

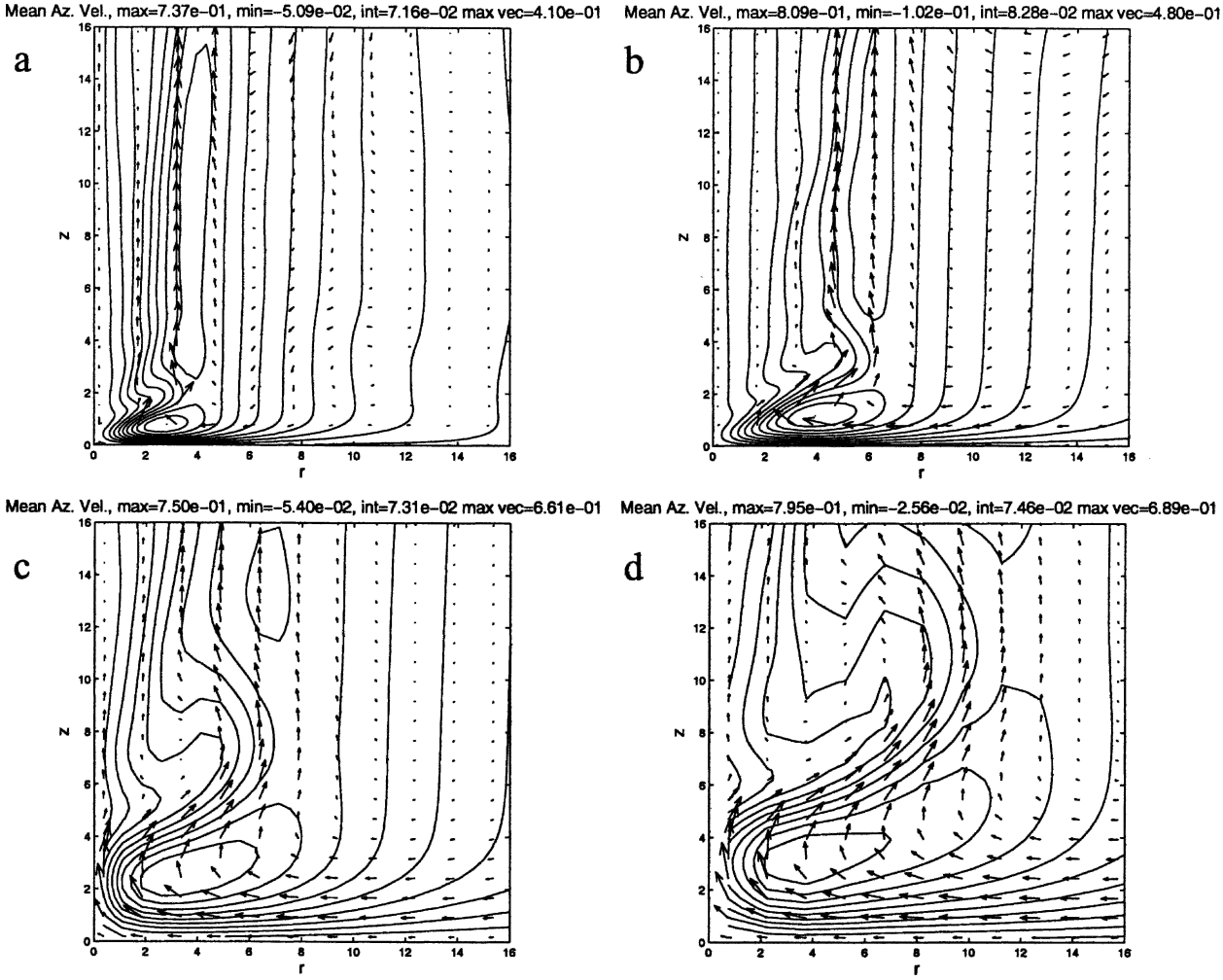

FIG. 3. Close ups of the corner flow for nondimensional simulations with variations to the environmental parameters: (a) $\Omega^* = 0.01$ s^{-1}; (b) $L_r^* = 1414$ m; (c) $\nu^* = 100$ m^2 s^{-1}; and (d) $L_r^* = 707$ m.

centered at $z_c^* = 2000$, 3000, and 4000 m, each with $L_r^* = L_z^* = 1000$ m. The lowest bubble contributed 1/6 of the total convective forcing, the middle bubble 1/2, and the upper bubble 1/3. Again, the low-level flow structure is nearly identical.

The controlling influence of Re_V on these types of vortices was demonstrated by Nolan and Farrell (1999). Here, we only show a few examples using the new scaling. For the results in Fig. 3, the parameters controlling Re_V have been changed. In Figs. 3a,b, Re_V has been doubled to a value of 100, by changing Ω^* to 0.01 s^{-1} or increasing L_r^* to 1414 m, respectively. The corner flow structures are nearly identical to each other, with significantly larger aspect ratios (defined as the ratio of the radius of the maximum winds to the altitude of the maximum winds), and nearly stagnant flow at the center axis. In Figs. 3c and 3d, Re_V has been halved to 25 by changing ν^* to 100 m^2 s^{-1} or L_r^* to 707 m, respectively. These last two corner flows are somewhat different in structure, but they both clearly show the low-swirl flow structure with a smaller aspect ratio and the maximum updraft at or very close to the center axis.

4. Conclusions

The nondimensionalization shown above is not a proof of the control of Re_V over the flow structure in tornado-like vortices simulated with a constant eddy viscosity model. This is clear from the presence of the additional dimensionless parameters γ and S_r, and by the small differences in the similar flow structures seen in Figs. 2 and 3. Nonetheless, the significance of Re_V is evident.

Real tornadoes are three-dimensional and highly turbulent. To what extent does the analysis presented here apply? The importance of the magnitude of the circu-

lation flowing into the vortex core in controlling the low-level structure in three-dimensional vortices has been established by both the laboratory models and three-dimensional numerical simulations (Fiedler 1998; Lewellen et al. 1997; Lewellen et al. 2000). However, these vortices were generated from purely axisymmetric environments. A remarkable feature of tornadoes, waterspouts, and dust devils is that the flow in and around the vortex core is often highly axisymmetric, even when the surrounding flow is highly asymmetric. Thus, the assumption that the radius of maximum winds occurs where fluid conserving its circulation achieves the expected CAPE velocity should still be valid; one would have to be more careful about how the far-field circulation is estimated. Estimates of vorticity and circulation in real mesocyclones have indeed been calculated from Doppler radar observations (Wakimoto and Liu 1998; Trapp 1999).

The diffusion of momentum and its loss into the surface are ultimately controlled by turbulence. For a turbulent flow over rough surfaces, the frictional parameter that, along with the circulation, controls the low-level flow structure would be the roughness length and its associated drag coefficient; this is consistent with observations and laboratory experiments (Church and Snow 1993, section 3.4). For turbulent flows, Re_V could perhaps be transformed into a similar parameter that is a ratio of the inflow circulation to some effective or bulk eddy viscosity, which is related to the turbulent kinetic energy, the surface roughness, and the shear of the resolved flow.

While the molecular vortex Reynolds number would be astronomically large in an atmospheric vortex, the scaling defined by (2.20)–(2.22) is still useful, as the maximum wind speeds and radius of maximum winds would still be $O(1)$, and the turbulence-dependent eddy viscosity would be scaled by the environmental circulation $\Gamma^* \approx \Omega^* L_r^{*2}$.

Acknowledgments. The author would like to thank Brian Farrell, Alexandre Chorin, Ann Almgren, John Bell, and Michael Montgomery for their support of previous studies, which led to the results presented here, and two anonymous reviewers, whose suggestions led to significant improvements. Dan Hodyss is also thanked for his comments on the manuscript. This work was supported by the University of Miami.

REFERENCES

Barenblatt, G. I., 1998: *Scaling, Self-Similarity, and Intermediate Asymptotics.* Cambridge University Press, 324 pp.

Bode, L., L. M. Leslie, and R. K. Smith, 1975: A numerical study of the boundary effects on concentrated vortices with application to waterspouts and tornadoes. *Quart. J. Roy. Meteor. Soc.*, **101**, 313–324.

Church, C. R., and J. T. Snow, 1993: Laboratory models of tornadoes. *The Tornado: Its Structure, Dynamics, Prediction, and Hazards.* C. Church et al., Eds. American Geophysical Union, 637 pp.

——, ——, G. L. Baker, and E. M. Agee, 1979: Characteristics of tornado-like vortices as a function of swirl ratio: A laboratory investigation. *J. Atmos. Sci.*, **36**, 1755–1776.

Davies-Jones, R. P., 1973: The dependence of core radius on swirl ratio in a tornado simulator. *J. Atmos. Sci.*, **30**, 1427–1430.

Dessens, J., 1972: Influence of ground roughness on tornadoes: A laboratory simulation. *J. Appl. Meteor.*, **11**, 72–75.

Fiedler, B. H., 1993: Numerical simulation of axisymmetric tornadogenesis in forced convection. *The Tornado: Its Structure, Dynamics, Prediction, and Hazards,* C. Church et. al., Eds., American Geophysical Union, 637 pp

——, 1994: The thermodynamic speed limit and its violation in axisymmetric numerical simulations of tornado-like vortices. *Atmos.–Ocean*, **32**, 335–359.

——, 1998: Wind-speed limits in numerically simulated tornadoes with suction vortices. *Quart. J. Roy. Meteor. Soc.*, **123**, 2377–2392.

Howells, P. C., R. Rotunno, and R. K. Smith, 1988: A comparative study of atmospheric and laboratory analogue numerical tornado-vortex models. *Quart. J. Roy. Meteor. Soc.*, **114**, 801–822.

Lewellen, D. C., W. S. Lewellen, and J. Xia, 2000: The influence of a local swirl ratio on tornado intensification near the surface. *J. Atmos. Sci.*, **57**, 527–544.

Lewellen, W. S., D. C. Lewellen, and R. Sykes, 1997: Large-eddy simulation of a tornado's interaction with the surface. *J. Atmos. Sci.*, **54**, 581–605.

Maxworthy, T., 1972: On the structure of concentrated, columnar vortices. *Atronaut. Acta*, **17**, 363–374.

Nolan, D. S., and B. F. Farrell, 1999: The structure and dynamics of tornado-like vortices. *J. Atmos. Sci.*, **56**, 2908–2936.

——, A. S. Almgren, and J. B. Bell, 2000: Studies of the relationship between the structure and dynamics of tornado-like vortices and their environmental forcing. Lawrence Berkeley National Laboratory Rep. LBNL-47554, 65 pp.

Rotunno, R., 1979: A study in tornado-like vortex dynamics. *J. Atmos. Sci.*, **36**, 140–155.

Trapp, R. J., 1999: Observations of nontornadic low-level mesocyclones and attendant tornadogenesis failure during VORTEX. *Mon. Wea. Rev.*, **127**, 1693–1705.

——, and R. P. Davies-Jones, 1997: Tornadogenesis with and without a dynamic pipe effect. *J. Atmos. Sci.*, **54**, 113–133.

Wakimoto, R. M., and C. Liu, 1998: The Garden City, Kansas, storm during VORTEX 95. Part II: The wall cloud and tornado. *Mon. Wea. Rev.*, **126**, 393–408.

Walko, R., and R. L. Gall, 1986: Some effects of momentum diffusion on axisymmetric vortices. *J. Atmos. Sci.*, **43**, 2137–2148.

Wan, C. A., and C. C. Chang, 1972: Measurements of the velocity field in a simulated tornado-like vortex using a three-dimensional velocity probe. *J. Atmos. Sci.*, **29**, 116–127.

Ward, N. B., 1972: The exploration of certain features of tornado dynamics using a laboratory model. *J. Atmos. Sci.*, **29**, 1194–1204.

Wurman, J., J. M. Straka, and E. N. Rasmussen, 1996: Fine-scale Doppler radar observations of tornadoes. *Science*, **272**, 1774–1777.